Article

Drug Transport across Porcine Intestine Using an Ussing Chamber System: Regional Differences and the Effect of P-Glycoprotein and CYP3A4 Activity on Drug Absorption

Yvonne E. Arnold [1], Julien Thorens [2,3], Stéphane Bernard [2] and Yogeshvar N. Kalia [1,*]

[1] School of Pharmaceutical Sciences, University of Geneva & University of Lausanne, CMU-1 rue Michel Servet, 1211 Geneva 4, Switzerland; Yvonne.Arnold@unige.ch

[2] Debiopharm International SA, Chemin Messidor 5-7, 1006 Lausanne, Switzerland; julienthorens@hotmail.com (J.T.); stephane.bernard@debiopharm.com (S.B.)

[3] Present address: Pharmacie des fins, 3 rue de Frontenex, 74000 Annecy, France

[*] Correspondence: yogi.kalia@unige.ch; Tel.: +41-022-379-3355

Abstract: Drug absorption across viable porcine intestines was investigated using an Ussing chamber system. The apparent permeability coefficients, $P_{app,pig}$, were compared to the permeability coefficients determined in humans in vivo, $P_{eff,human}$. Eleven drugs from the different Biopharmaceutical Classification System (BCS) categories absorbed by passive diffusion with published $P_{eff,human}$ values were used to test the system. The initial experiments measured $P_{app,pig}$ for each drug after application in a Krebs–Bicarbonate Ringer (KBR) buffer and in biorelevant media FaSSIF V2 and FeSSIF V2, mimicking fasted and fed states. Strong sigmoidal correlations were observed between $P_{eff,human}$ and $P_{app,pig}$. Differences in the segmental $P_{app,pig}$ of antipyrine, cimetidine and metoprolol confirmed the discrimination between drug uptake in the duodenum, jejunum and ileum (and colon); the results were in good agreement with human data in vivo. The presence of the P-gp inhibitor verapamil significantly increased $P_{app,pig}$ across the ileum of the P-gp substrates cimetidine and ranitidine ($p < 0.05$). Clotrimazole, a potent CYP3A4 inhibitor, significantly increased $P_{app,pig}$ of the CYP3A4 substrates midazolam, verapamil and tamoxifen and significantly decreased the formation of their main metabolites. In conclusion, the results showed that this is a robust technique to predict passive drug permeability under fasted and fed states, to identify regional differences in drug permeability and to demonstrate the activity of P-gp and CYP3A4.

Keywords: intestinal permeability; regional drug absorption; Ussing chamber; biorelevant media; P-gp; CYP3A4

1. Introduction

Methods to predict intestinal drug absorption in humans in vivo range from purely in silico computational techniques to preclinical animal studies in vivo. In vitro tests range from relatively simple solubilization or permeation studies to more advanced systems, mimicking several steps or even the complete passage through the gastrointestinal tract [1–7]. High-throughput methods (e.g., PAMPA or Caco-2 cell lines) are frequently used in early, preclinical stages. The monolayer cell culture system is limited by the absence of a full physiological membrane and the specific properties of the individual cell types present in the different segments of the intestine. These models are usually used to evaluate the permeability of the API alone since they are not sufficiently robust to support either biorelevant media or "real" formulations. Indeed, to better approach the physiological

conditions, mucus-producing HT29-MTX cells and M cells inducing Raji B cells were introduced into the Caco-2 monolayer [8–13]. Although in vivo studies cannot necessarily provide insight into regional differences in drug absorption, this has been attempted to be addressed in rats by the single-pass intestinal perfusion technique or, with appropriate adjustments, the closed-loop Doluisio method [14].

In order to have comprehensive permeability data for the selection of lead drug candidates and to predict the absorption in humans in vivo, it is crucial to have a physiologically and anatomically similar model that can address the following points: (i) the identification of absorption sites (crucial for modified-release formulations and poorly soluble compounds), (ii) a full physiological membrane evaluation (including mucus layer), (iii) the influence of excipients on drug permeability, (iv) drug metabolism in epithelial cells, (v) the effect of active transporters and efflux systems, and (vi) the drug/drug interactions: These will determine the relevance of the model for humans, i.e., its predictive power.

One approach is to use an Ussing chamber system, which enables transport experiments to be performed using viable intestinal tissue ex vivo [15–21]; tissue integrity is monitored by the continuous measurement of transepithelial resistance. Human intestine is obviously the most suitable tissue for ex vivo evaluations, and there have been some studies over the last twenty years [22–27]. Much work was done by the Drug Metabolism and Pharmacokinetics group at AstraZeneca R&D, which published a landmark paper in 2013 that compiled 15 years of data on drug absorption focusing mainly on transport across the human jejunum and colon and the effect of pre-systemic metabolism and efflux transporters [28]. However, the availability of viable human intestine is extremely limited-samples are usually obtained from patients suffering from malignancies [23,26,28,29]. To circumvent this, rat intestines have been the traditional animal model of choice for ex vivo/in vivo permeation studies [24,30–32]. However, it has a number of limitations, including differences in intestinal morphology and other distinct physiological differences that can make extrapolation to humans difficult [33]. Although the major drug transporters in humans and rats are in good correlation, the enzyme expression between human and rat intestines is different: For example, rat intestine displays pre-systemic cytochrome P450 activity, but this does not correlate to the activity in the human intestine [34]. In addition to the scientific issues concerning relevance, ethical concerns can also be cited with the use of rats as they have to be sacrificed for such evaluations.

Like humans, pigs are large omnivorous mammals, and porcine intestine shows greater similarities to human intestine than the intestinal tissue from other animals [33–36]. For nutritional studies, the porcine model is known to be superior to other non-primate animal models: Despite some anatomic differences, the physiology of digestion and the associated metabolic processes are much alike between humans and pigs [37]. The gross anatomical features of the GI tract of pigs and humans are similar, although the divisions between the duodenum, jejunum and ileum are not as distinct in porcine small intestine [35]. Microscopically, the intestinal villus structure and component epithelial cell types are very alike, and the pH variations of the different regions of the gastrointestinal tract in pigs and human are, again, similar [33].

At a molecular level, the metabolic activities for Phase 1 and Phase 2 enzymes in humans and pigs are closely related [34]. Porcine intestine appears to possess a high cytochrome P450 CYP3A activity, and there is more homology between human and porcine CYP3A enzymes than with those in the rat [38,39]. In both humans and pigs, P-gp is coded by a single gene (ABCB1 (ATP-binding cassette B1) or MDR1 (multidrug resistance 1)) (cf. two P-gp homologues in rats). The alignment of the porcine and human P-gp sequences resulted in a homology of 90.8%, with a high homology in the predicted transmembrane domains known to be important for substrate binding [40]. Moreover, P-gp expression was shown to increase from the proximal to distal regions in the small intestine of Yucatan micropigs—as is the case in humans [41,42]. Multidrug-resistance-associated protein (MRP2), breast cancer-resistant protein (BCRP), peptide transporter-1 (PepT1) and organic anion-transporting polypeptide (OATP) are present in porcine intestine [34].

The objective of the present study was to demonstrate that the Ussing chamber system with porcine intestine could be a useful surrogate to predict intestinal absorption in humans. Reports describing the use of porcine intestine to model drug absorption using the Ussing chamber or related systems and with diffusion cells are scarce [43–55], e.g., indeed, Ussing chamber investigations have only been performed on the uptake of polyphenols present in apples [43] and in coffee [44]. To our knowledge, the only detailed investigation to date into the feasibility of using porcine intestine to predict human intestinal absorption employed a diffusion cell-based system with a view to enable the development of a "medium throughput" technique [45].

The systematic approach employed in the present study was similar to that used by Sjöberg et al. with an extension to include the use of physiologically relevant media [28]. The specific aims were (i) to investigate the absorption of a training set of 11 molecules across viable porcine intestine from a Krebs–Bicarbonate Ringer (KBR) buffer and, with a view approaching more physiologic conditions, from the biorelevant media Fasted State Simulated Intestinal Fluid Version 2 (FaSSIF V2) and Fed State Simulated Intestinal Fluid Version 2 (FeSSIF V2) and to correlate the experimental $P_{app,pig}$ with $P_{eff,human}$ values determined in humans in vivo; (ii) to demonstrate the ability of the model to detect the regional variation in drug absorption in the different segments of the small intestine (i.e., duodenum, jejunum and ileum)—furthermore, uptake in the colon was also evaluated—(iii) to determine $P_{app,pig}$ of the P-gp substrates, cimetidine and ranitidine, in the presence and absence of the P-gp inhibitor, verapamil, to demonstrate that the efflux transporter retained its activity in the porcine intestine ex vivo; and likewise, (iv) to determine $P_{app,pig}$ of the CYP3A4 substrates, midazolam, tamoxifen and verapamil, in the presence and absence of the potent CYP3A4 inhibitor, clotrimazole, to confirm that the enzyme retained activity. Furthermore, the respective metabolites, hydroxymidazolam, N-desmethyl-tamoxifen and norverapamil, were also quantified.

2. Materials and Methods

2.1. Chemicals

Antipyrine, cimetidine, clotrimazole, N-desmethyl-tamoxifen hydrochloride, furosemide, hydrochlorothiazide, ketoprofen, maleic acid, (+/−)-metoprolol-(+)-tartrate, (+/−)-norverapamil hydrochloride, piroxicam, tamoxifen, terbutaline hemisulfate and (+/−)-verapamil hydrochloride 99% were purchased from Sigma-Aldrich (St. Louis, MO, USA); (+/−)-propranolol hydrochloride and ranitidine hydrochloride were obtained from Alfa Aesar GmbH & Co KG (Karlsruhe, Germany), and carbamazepine was purchased from Acros Organics (New Jersey, USA). Midazolam and α-hydroxymidazolam were purchased from Lipomed AG (Arlesheim, Switzerland), and agar, calcium chloride dihydrate, glucose hydrate, magnesium chloride hexahydrate, potassium chloride, sodium chloride, sodium hydroxide, sodium phosphate monobasic and sodium hydrogencarbonate were obtained from Hänseler AG (Herisau, Switzerland). Sodium taurocholate was purchased from Prodotti Chimici e Alimentari S.p.A., (Basaluzzo, Italy) and lecithin (grade EPCS > 98% phospholipids) was obtained from Lipoid GmbH (Ludwigshafen, Germany).

2.2. Porcine Intestinal Tissue

Porcine intestinal tissue from 6-month-old female Swiss noble pigs (weight: 100–120 kg) was supplied by two local abattoirs (Abattoir de Meinier; Meinier, Switzerland and Abattoir de Loëx; Bernex, Switzerland) and was collected immediately after slaughter. In order to remove the luminal debris, the tissue was rinsed with ice-cold KBR (120 mM NaCl, 5.5 mM KCl, 2.5 mM $CaCl_2$, 1.2 mM $MgCl_2$, 1.2 mM NaH_2PO_4, 20 mM $NaHCO_3$ and 11 mM glucose; pH 7.4) [56]. During transport from the slaughterhouse to the laboratory, the tissue was stored in ice-cold KBR and constantly bubbled with a 95% O_2/5% CO_2 gas mixture (PanGas AG; Dagmersellen, Switzerland).

Once in the laboratory, the intestinal tissue was prepared using previously published protocols [46,57]. Briefly, the intestine was opened along the mesenteric border and rinsed with

ice-cold KBR. The muscle layer was carefully removed using a scalpel and fine forceps. The remaining tunica mucosa and submucosa were cut into segments of approximately 1.5 cm^2. Areas including Peyer's patches were avoided. During the whole procedure, which took 5–10 min, the tissue was stored in ice-cold KBR and constantly bubbled with a gas mixture of 95% O_2/5% CO_2.

2.3. Ussing Chamber Setup and Procedures for Intestinal Absorption Experiments

A six Ussing chamber system coupled to a VCC MC6 MultiChannel Voltage–Current Clamp (Physiologic Instruments; San Diego, CA, USA) with a heating block and six input modules with integral dummy membranes was used for the permeation studies. A circulating water bath (ED-5, Julabo GmbH, Seelbach, Germany) was used to regulate the temperature. The Ussing chambers were set up using the method reported by Neirinckx et al. [46]. First, the Ag/AgCl electrodes were put in tips containing a congealed mixture of 3% agar in 3 M KCl. Then, the electrodes were inserted into the Ussing chambers, and the donor and acceptor compartments were filled with preheated KBR (38°C). The buffer solution was constantly bubbled with a 95% O_2/5% CO_2 gas mixture; in addition to oxygenating the tissue, this ensured mixing and circulation of the buffer in the two compartments. Any voltage difference between the electrodes and the transepithelial electrical resistance due to the buffer solution was eliminated. The chambers were emptied, the intestinal tissue was mounted on the sliders with an exposed surface area of 1.26 cm^2 and the sliders were inserted into the Ussing chambers. The intestine was mounted in the Ussing chamber 45 min after harvesting from the animal. KBR (7 mL) was added to the donor and acceptor compartments and left to equilibrate for 30 min, at which point both the donor and acceptor compartments were emptied and the acceptor phase was replaced with the same volume of fresh KBR (7 mL) so as to minimize the potential impact of endogenous material released during the 30 min equilibration period.

The composition of the solution in the donor compartment was dependent on the experiments: (i) in the first study into passive drug absorption, each API from the training set of 11 molecules (Table 1) was dissolved in KBR (7 mL) to prepare a 100 µM solution; (ii) in the second series of experiments, which investigated the effect of using fasted state biorelevant media on drug absorption, each API (100 µM) was dissolved in FaSSIF V2 (7 mL; 68.62 mM NaCl, 34.8 mM NaOH, 19.12 mM maleic acid, 3 mM Na taurocholate and 3 mM lecithin; pH 6.5) [58]; (iii) in the third series, which investigated the effect of fed state conditions on drug uptake, the API was dissolved in FeSSIF V2 (7 mL; 125.5 mM NaCl, 69.9 mM NaOH, 55.02 mM maleic acid, 10 mM Na taurocholate, 2 mM lecithin, 0.8 mM glycerol monooleate and 0.8 mM sodium oleate; pH 5.8) [58].

Table 1. The chemical structures and physicochemical properties of the drug molecules tested using the Ussing chamber system.

API	MW (g/mol)	log P	log D [59] Octanol/H_2O pH 7.4	pH 6.5	pH 5.5	Solubility (n = 3) (mg/mL) KBR	FaSSIF V2	FeSSIF V2	Study
BCS I									
Antipyrine (1) $C_{11}H_{12}N_2O$	188.23	0.38	0.6	0.6	0.6	103.00 ± 54.61	261.10 ± 132.29	564.44 ± 83.12	Passive [b] Regional [c]
Ketoprofen (2) $C_{16}H_{14}O_3$	254.28	3.12	0.1	0.8	1.8	2.82 ± 0.62	6.73 ± 2.70	6.37 ± 1.52	Passive
(+/−)-Metoprolol (3) $C_{15}H_{25}NO_3$	267.36	1.88	0.0	−0.5	−0.6	298.03 ± 13.86	43.85 ± 15.81	380.69 ± 33.79	Passive Regional
Midazolam $C_{18}H_{13}ClFN_3$	325.77	3.89	3.0 [a]	3.6 [a]	3.9 [a]	n.a.	n.a.	n.a.	CYP3A4 [d]
Propranolol (4) $C_{16}H_{21}NO_2$	259.34	3.48	1.4	0.9	0.7	158.69 ± 4.34	247.53 ± 7.47	222.57 ± 2.00	Passive
Verapamil $C_{27}H_{38}N_2O_4$	454.60	3.79	3.8 [a]	3.8 [a]	3.8 [a]	1.04 ± 0.09	5.60 ± 1.04	17.60 ± 0.98	CYP3A4
BCS II									
Carbamazepine (5) $C_{15}H_{12}N_2O$	236.27	2.1	2.45	2.45	2.45	0.20 ± 0.02	0.32 ± 0.01	0.73 ± 0.01	Passive
Naproxen (6) $C_{14}H_{14}O_3$	230	3.18	0.3	1.1	2.1	4.51 ± 0.04	14.59 ± 1.19	13.00 ± 2.37	Passive
Piroxicam (7) $C_{15}H_{13}N_3O_4S$	331.35	3.06	0.2 [a]	1.1 [a]	2.0 [a]	0.43 ± 0.02	0.29 ± 0.02	0.06 ± 0.00	Passive
Tamoxifen $C_{26}H_{29}NO$	371.51	5.93	5.6 [a]	5.9 [a]	5.9 [a]	23.32 ± 1.54	32.19 ± 0.42	27.87 ± 0.66	CYP3A4

Table 1. *Cont.*

API	MW (g/mol)	log *P*	log *D* [59] Octanol/H$_2$O pH 7.4	pH 6.5	pH 5.5	KBR	Solubility (*n* = 3) (mg/mL) FaSSIF V2	FeSSIF V2	Study
BSC III									
Atenolol (8) C$_{14}$H$_{22}$N$_2$O$_3$	365.40	0.75	−2.0	−2.0	−2.0	35.57 ± 7.29	33.73 ± 2.06	41.28 ± 1.16	Passive
Cimetidine C$_{14}$H$_{22}$N$_2$O$_3$	252.34	0.40	0.4 [a]	0.4 [a]	0.4 [a]	5.65 ± 0.13	5.88 ± 0.26	0.36 ± 0.26	Regional P-gp [e]
Ranitidine C$_{14}$H$_{22}$N$_2$O$_3$	314.40	0.27	0.2 [a]	0.3 [a]	0.3 [a]	19.64 ± 2.78	15.89 ± 1.47	807.51 ± 70.47	P-gp
Terbutaline (9) C$_{14}$H$_{22}$N$_2$O$_3$	225.28	0.9	−1.4	−1.3	−1.3	213.73 ± 15.18	372.59 ± 18.86	305.07 ± 124.48	Passive
BCS IV									
Furosemide (10) C$_{12}$H$_{11}$ClN$_2$O$_5$S	330.74	2.03	−0.9	−0.5	0.4	5.62 ± 0.10	24.90 ± 2.84	19.68 ± 2.59	Passive
Hydrochlorothiazide (11) C$_7$H$_8$ClN$_3$O$_4$S$_2$	297.74	−0.16	−0.2	−0.2	−0.2	0.81 ± 0.17	1.18 ± 0.14	1.04 ± 0.19	Passive

[a] The log *D* value was not taken from Reference [54] but was calculated using the following equation: $\log D = \log P + \log(\frac{1}{1+10^{pH-pKa}})$; [b] Passive: the drug used to study passive drug permeation from KBR and biorelevant media; [c] Regional: the drug used to study drug permeation in different intestinal segments; [d] CYP3A4: the drug used to study CYP3A4 activity; [e] P-gp: the drug used to study P-gp activity.

For the experiments investigating the effect of P-gp, verapamil hydrochloride (a known P-gp inhibitor) was added to the formulation in the donor compartment, again at 100 μM and similar to the concentration reported in the literature [60]. For the study investigating the activity of CYP3A4 present in the intestinal membrane, the experiments were performed in the presence/absence of clotrimazole—a potent CYP3A4 inhibitor (K_i = 18 nM)—again at 100 μM [61]. Given the experimental setup, all experiments were performed in sextuplicate.

The cumulative drug permeation across the intestinal epithelium was determined by taking aliquots (400 μL) from the acceptor compartment every 20 min (t = 20, 40, 60, 80, 100 and 120 min); the volume removed was replaced with a fresh buffer. During the experiment, the viability of the intestinal tissue was monitored by measuring the variation of the voltage during the intermittent application of a 50 μA current pulse (duration 200 ms) applied every minute. Using Ohm's law, the transepithelial electrical resistance was calculated and used as a measure for tissue viability. Preliminary studies were performed to define the threshold transepithelial electrical resistance value below which the tissue integrity was considered to be impaired or not viable. Based on these measurements, tissues with a transepithelial electrical resistance below 15 Ω.cm^2 were considered not to be viable or intact and were not used for the calculation of the permeability coefficients.

Upon completion of the experiment (t = 120 min), in addition to the sample from the acceptor, a 400 μL aliquot was withdrawn from the donor compartment. The intestinal slices were cut into small pieces and extracted for 6 h using the mobile phase used for the UHPLC-MS/MS analytical method (see below). This enabled the amount of API retained in the intestinal tissue to be determined. Prior to analysis, all samples were centrifuged for 10 min at 14 000 rpm using an Eppendorf Centrifuge 5804 (Vaudaux-Eppendorf AG; Schönenbuch, Switzerland).

2.4. Analytical Methods

The samples were analyzed using UHPLC-MS/MS. The system consisted of a Waters ACQUITY UPLC$^®$ core system and a Waters XEVO$^®$ TQ-MS tandem quadrupole mass spectrometer (Milford, MA, USA). Chromatographic separation was achieved using an ACQUITY UPLC$^®$ BEH C18 column, 1.7 μm, 25 × 2.1 mm, attached to an ACQUITY UPLC$^®$ BEH C18 Van Guard™ Pre-column, 1.7 μm, 5 × 2.1 mm. Tandem mass spectrometry was performed in the multiple reaction monitoring (MRM), mode and the majority of the APIs (Supplementary Material, Table S1) were analyzed with positive ion electrospray ionization (ESI). Furosemide, hydrocholorothiazide, ketoprofen and piroxicam were analyzed with negative ESI (Table S1). The complete details of the isocratic UHPLC-MS/MS methods are reported in the Supplementary Material (Table S1 and Table S2). Data acquisition was done using the MassLynx™ software, version 4.1.

2.5. Data Analysis

2.5.1. Permeability Calculations

The apparent permeability coefficient for transport across the porcine intestinal tissue ($P_{app,pig}$) was calculated using the following equation:

$$P_{app,\ pig} = \frac{dc}{dt} \times \frac{V}{A \times C_0} \left(\frac{cm}{s} \right) \tag{1}$$

where *dc/dt* is the change in the acceptor concentration calculated from the slope of the concentration–time curve between 20 and 80 min, *V* is the buffer volume in the donor compartment, *A* is the exposed surface area (1.26 cm^2) and C_0 is the initial concentration of the API in the donor compartment [62].

2.5.2. Data Fitting

The experimental permeability values $P_{app,pig}$ were fitted to the in vivo permeability $P_{eff,human}$ values using a four parameter logistic equation (SigmaPlot software, version 12.5—Systat Software Inc.; San Jose, CA, USA) as used by Sjöberg et al., where y_0 is the minimum value of $P_{eff,human}$, X_{50} is the $P_{app,pig}$ when $P_{eff,human}$ is at half the maximum value, a is a scaling factor and b is the slope factor [28].

$$P_{eff,\, human} = y_0 + \frac{a}{1 + \left(\frac{P_{app,\, pig}}{X_{50}}\right)^b} \tag{2}$$

2.5.3. Evaluation of the Relative Contributions of Drug Deposition and Permeation During Intestinal Transport: The Transport Index (TI)

Conventional approaches to evaluate intestinal drug absorption use the permeability coefficient as the reference parameter. This does not take into account drug retention in the membrane. The quantification of drug deposition in addition to permeation is routinely carried out in investigations into the transport of drugs across other biological membranes [63–66]. In this context, Miyake et al. recently introduced the concept of the transport index (*TI*) to reflect the sum of the amounts accumulated in the intestine (Q_{DEP}) and permeated across the tissue (Q_{PERM}) as a percentage of the amount applied in the donor compartment [27,67]. This is analogous to a "delivery efficiency", which is again used in topical and transdermal delivery studies to indicate the fraction of drugs delivered from a formulation into or across the skin [68–70].

In the conditions used in the present study, Q_{DEP} and Q_{PERM} are calculated as follows:

$$Q_{DEP} = \frac{m_{int\, 2h}}{m_{donor\, 0h}} \times 100 \; (\%) \tag{3}$$

$$Q_{PERM} = \frac{m_{acc\, 2h}}{m_{donor\, 0h}} \times 100 \; (\%) \tag{4}$$

where $m_{int\, 2h}$ and $m_{acc\, 2h}$ represent the amounts deposited in and permeated across the intestine at 2 h and $m_{donor\, 0h}$ is the amount present in the donor compartment at $t = 0$.

2.6. Statistical Analysis

The data were expressed as the mean $\pm$ SD. The results were evaluated statistically using analysis of variance (one-way ANOVA) followed by Bonferroni's multiple comparisons test or Student's *t*-test. The level of significance was fixed at $\alpha = 0.05$.

3. Results and Discussion

3.1. Intestinal Absorption of Drugs from KBR and FaSSIF V2 and FeSSIF V2

The first part of the study involved the validation of the setup. This was done by determining the $P_{app,pig}$ of 11 drugs from the four BCS categories (seven high and four low permeability) formulated in KBR and in FaSSIF V2 and FeSSIF V2 followed by a comparison to the $P_{eff,human}$ reported in the literature (Tables 1 and 2). The mean initial transepithelial resistance of the jejunum, $41.77 \pm 13.78 \; \Omega.cm^2$ ($n = 155$), was similar to the resistance of the human intestine (duodenum/jejunum; $34 \pm 12 \; \Omega.cm^2$) [28], and its monitoring for the duration of the experiment reported on the tissue viability in the presence of KBR and, importantly, the effect of biorelevant media in the donor compartment. The ability to use biorelevant media that simulate more physiological conditions is a major advantage of this system since it enables a better approximation of the food effects on drug permeation [71]; this can be difficult with Caco-2 cells due to the cytotoxic effects [72] (necessitating the development of more complex systems [13,73–75]). As seen with other ex vivo models, the $P_{app,pig}$ values were, in general, smaller than the effective permeability $P_{eff,human}$ determined in humans in vivo with the Loc-I-Gut single-pass

perfusion technique [76]. This can be explained by the differences between the physiological and experimental conditions. For example, $P_{app,pig}$ (and the apparent permeability coefficients with other species) calculated from Ussing chamber data ex vivo are derived from the drug concentration gradient observed in the acceptor compartment as the amount permeated across a small piece of intestine with a defined area gradually increasing with time. They do not take into account the amount of drug that is retained in the intestinal tissue, which can be significant for certain molecules (Table 1). In contrast, $P_{eff,human}$ calculated in vivo using the Loc-I-Gut technique is dependent upon the difference in concentration over a given length of tissue:

$$P_{eff,\,human} = \frac{Q_{in}}{A}\,ln\left(\frac{C_{out}}{C_{in}}\right) \qquad (5)$$

where Q_{in} is the input rate, C_{in} and C_{out} are the drug concentrations at the start and end of the intestinal segment and A is the surface area for absorption. Thus, any process contributing to the loss of the drug from the intestinal fluid will contribute to an increase in $P_{eff,human}$. The surface area for absorption in the Loc-I-Gut model has typically been modelled as a smooth, flat cylinder, ignoring the presence of villi and microvilli, which significantly increase the effective surface area through which drug absorption can occur. A correction of the absorption area to take into account the presence of the additional surface provided by the villi/microvilli would result in a new estimate for the area, which, by definition, would be greater than that of the smooth cylinder and, hence, reduce the value of $P_{eff,human}$. The impact of this additional surface area was recently shown by Olivares-Morales et al., who demonstrated that the estimated $P_{eff,human}$ changed dramatically upon including a physiologically relevant estimate of the intestinal surface area available for drug absorption [77]. A correction of the surface area decreased $P_{eff,human}$ and brought the values closer to the permeability coefficients reported ex vivo. The comparison of these corrected $P_{eff,human}$ and the $P_{app,pig}$ obtained here using the Ussing chamber system shows excellent agreement (Table 2).

Table 2. The apparent permeability coefficients for passive absorption across porcine intestine, $P_{app,pig}$, from KBR and the biorelevant media FaSSIF V2 and FeSSIF V2 and the Q_{DEP} and Q_{PERM} values determined with viable porcine intestine ex vivo (n ≥ 3): The effective permeability coefficients[a,b] for absorption in vivo in humans, $P_{eff,\,human}$, are given for comparison.

Drug	$P_{app,pig}$ Ex Vivo (10^{-6} cm/s)			$P_{eff,human}$[a] In Vivo (10^{-6} cm/s)	$P_{eff,human}$[b] In Vivo (10^{-6} cm/s)	Q_{DEP} (%) KBR	Q_{PERM} (%) KBR	(n)[c]	Q_{DEP} (%) FaSSIF V2	Q_{PERM} (%) FaSSIF V2	(n)[c]	Q_{DEP} (%) FeSSIF V2	Q_{PERM} (%) FeSSIF V2	(n)[c]
	KBR (*n*)	FaSSIF V2 (*n*)	FeSSIF V2 (*n*)											
BCS I														
(1) Antipyrine	8.06 ± 7.91 (10)	6.18 ± 2.18 (4)	7.47 ± 0.95 (3)	560 ± n.a. [31]	19–29 [77]	0.72 ± 0.20	2.18 ± 0.53	(6)	1.07 ± 0.22	0.33 ± 0.16	(4)	2.90 ± 0.26	1.03 ± 0.28	(3)
(2) Ketoprofen	26.31 ± 1.49 (3)	6.34 ± 2.63 (5)	6.42 ± 2.44 (4)	870 ± n.a. [31]	29–45 [77]	11.57 ± 2.65	6.25 ± 0.92	(6)	4.49 ± 1.61	0.90 ± 0.46	(5)	0.37 ± 0.08	0.97 ± 0.54	(4)
(3) Metoprolol	10.64 ± 2.92 (3)	7.62 ± 1.41 (3)	5.79 ± 1.38 (3)	850 ± n.a. [31]	5.2–7.9 [77]	0.28 ± 0.04	0.18 ± 0.05	(6)	0.12 ± 0.03	0.89 ± 0.19	(3)	0.22 ± 0.01	0.74 ± 0.08	(3)
(4) Propranolol	6.01 ± 3.41(5)	0.71 ± 0.24 (3)	0.93 ± 0.55 (3)	280 ± 130 [31]	9.3–14 [77]	0.35 ± 0.06	0.04 ± 0.05	(6)	4.17 ± 0.15	0.27 ± 0.03	(3)	1.61 ± 0.57	0.27 ± 0.30	(3)
BCS II														
(5) Carbamazepine	7.81 ± 5.69 (16)	5.97 ± 0.52 (4)	4.26 ± 0.96 (6)	430 ± n.a. [31]	-	1.44 ± 0.16	2.39 ± 0.42	(6)	n.a.	n.a.	-	3.45 ± 0.52	0.58 ± 0.22	(6)
(6) Naproxen	12.14 ± 4.83 (3)	9.33 ± 3.36 (3)	45.47 ± 7.97 (5)	850 ± n.a. [31]	27–42 [77]	n.a.	n.a.	-	n.a.	n.a.	-	4.74 ± 1.04	8.11 ± 1.22	(5)
(7) Piroxicam	8.93 ± 2.03 (3)	10.83 ± 3.70 (3)	5.14 ± 0.78 (4)	665 ± n.a. [31]	-	4.12 ± 0.15	2.52 ± 0.70	(3)	5.63 ± 0.26	2.32 ± 0.79	(3)	0.21 ± 0.04	1.13 ± 0.46	(5)
BCS III														
(8) Atenolol	3.05 ± 0.73 (6)	3.70 ± 1.28 (6)	4.53 ± 1.71 (5)	20 ± n.a. [31]	1.8–2.8 [77]	7.38 ± 3.11	0.67 ± 0.13	(6)	0.25 ± 0.06	0.48 ± 0.09	(6)	0.55 ± 0.11	0.61 ± 0.12	(5)
(9) Terbutaline	5.33 ± 1.95 (17)	4.47 ± 0.62 (5)	3.30 ± 0.68 (6)	30 ± 30 [78]	1.7–2.6 [77]	0.52 ± 0.11	0.66 ± 0.22	(6)	39.47 ± 2.51	0.54 ± 0.29	(5)	0.04 ± 0.00	0.39 ± 0.10	(6)
BCS IV														
(10) Furosemide	1.69 ± 0.89 (16)	3.34 ± 1.46 (4)	3.83 ± 0.77 (6)	5 ± n.a. [31]	1–1.6 [77]	n.a.	n.a.	-	2.22 ± 0.17	0.43 ± 0.09	(4)	1.52 ± 0.24	1.38 ± 0.24	(6)
(11) Hydrochlorothiazide	2.88 ± 2.84 (17)	0.2 ± 0.25 (3)	1.37 ± 0.53 (6)	4 ± n.a. [31]	-	n.a.	n.a.	-	0.22 ± 0.11	0.11 ± 0.05	(3)	0.74 ± 0.09	0.23 ± 0.08	(6)

[a] $P_{eff,human}$ determined using the Loc-I-Gut method was performed in living humans. A jejunal segment of 10 cm was isolated and perfused with a solution with a known drug concentration. The difference in drug concentrations across the isolated segment was used to estimate the drug absorption, and this amount together with the assumption of a cylindrical surface area for uptake enabled the estimation of $P_{eff,human}$; [b] $P_{eff,human}$ calculated using the Loc-I-Gut method was performed in living humans but with the inclusion of physiological estimates of the surface area for absorption [77]; [c] Number of replicates.

The $P_{eff,human}$ (uncorrected)$/P_{app,pig}$ ratios for high permeability drugs were approximately 20-fold greater than those for low permeability drugs. The permeation surface for high permeability drugs, normally absorbed via the transcellular pathway, is larger compared to that of low permeability drugs, which are absorbed by the paracellular pathway. Therefore, a reduction in or a lack of blood flow, motility or lymphatic drainage in ex vivo experiments influences high permeability drugs much more than low permeability drugs—hence, their higher $P_{eff,human}$ /$P_{app,pig}$ ratios.

In a next step, the published $P_{eff,human}$ values were plotted against the ln $P_{app, pig}$ values for the three experimental setups KBR/KBR, FaSSIF V2/KBR, and FeSSIF V2/KBR (Figure 1). In every case, strong sigmoidal correlations (R^2 = 0.97 for KBR/KBR, R^2 = 0.91 for FaSSIF V2/KBR and R^2 = 0.76 for FeSSIF V2/KBR) were obtained and it was possible to distinguish clearly between high and low permeability drugs. The data were fitted using a four parameter logistic equation (see Section 2.5.2) [28]; in general, $P_{app, pig}$ decreased going from KBR to FaSSIF V2 and FeSSIF V2, and the correlation curves were translated to the left. The quality of the fit decreased going from KBR/KBR to FeSSIF V2/KBR. A trend towards a decreased permeability with an increasing concentration of sodium taurocholate and lecithin in the biorelevant media was found. This was in good agreement with previous findings, where it was observed that, depending on the drug characteristics, permeability decreased with an increasing concentration of solubility enhancers since poorly water soluble drugs were increasingly solubilized in the micelles, and therefore, less free drug was available for permeation [79,80]. Thus, the composition of FeSSIF V2 makes it more likely to influence the solubility and absorption of certain drugs, and this additional complexity might affect the quality of the correlation.
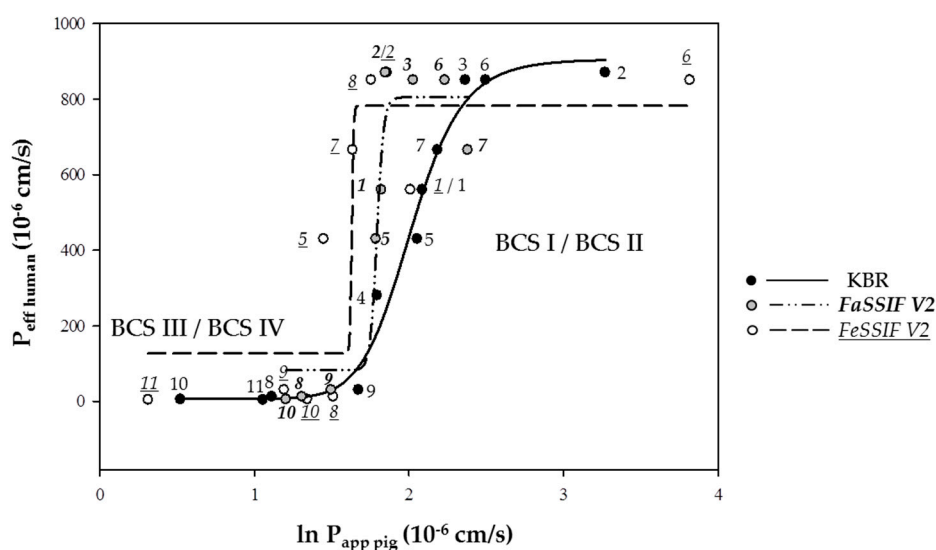

Figure 1. The correlation between the effective permeability coefficient in vivo, $P_{eff,human}$ (literature values derived assuming smooth cylindrical representation of the surface area for absorption) and the permeability coefficient calculated using porcine intestine ex vivo and the Ussing chamber technique ($P_{app,pig}$): The drug absorption was tested using KBR, and the biorelevant media, FaSSIF V2, and FeSSIF V2. BCS I/II (High permeability drugs): 1. Antipyrine, 2. Ketoprofen, 3. Metoprolol, 4. Propranolol, 5. Carbamazepine, 6. Naproxen and 7. Piroxicam; BCS III/IV (Low permeability drugs): 8. Atenolol, 9. Terbutaline, 10. Furosemide and 11. Hydrochlorothiazide (for n, see Table 2). A 100 µM solution of each drug was prepared in (i) KBR, (ii) FaSSIF V2 and (iii) FeSSIF V2. A four parameter logistic model was used to derive the fit between $P_{eff,human}$ and $P_{app,pig}$ (see Section 2.5.2) [28].

As the $P_{eff,human}$ values are obtained for more molecules, further experiments can be carried out with the porcine intestine to determine the corresponding $P_{app,pig}$ and so to expand the dataset.

3.2. Segmental Intestinal Drug Permeation: Regional Variations in Drug Uptake

Physiological factors such as variation of the surface, "tightness" of the tight junctions, variable expression of uptake and efflux transporters as well as enzymes can result in regional differences in drug absorption [81]. The identification of segmental drug permeation differences at an early stage can be advantageous since it can be used to optimize formulation development. Interestingly, the mean transepithelial resistances of the four intestinal segments at the start of the experiments were found to be in the same range: $57.33 \pm 20.66 \ \Omega.cm^2$ ($n = 14$) for the duodenum, $41.77 \pm 13.79 \ \Omega.cm^2$ ($n = 155$) for the jejunum, $40.85 \pm 15.08 \ \Omega.cm^2$ ($n = 31$) for the ileum and $35.71 \pm 16.56 \ \Omega.cm^2$ ($n = 18$) for the colon. The ability of the model to identify segmental differences in intestinal drug permeation was tested by determining $P_{app,pig}$ of antipyrine and metoprolol (two high permeability drugs; BCS I) and cimetidine (low permeability drug; BCS III) across the duodenum, jejunum, ileum and colon (Figure 2 and Table 3). Due to their lipophilicity, antipyrine and metoprolol are absorbed passively via the transcellular pathway [82]. Cimetidine, in contrast, is transported by the paracellular pathway, and it is also a P-gp substrate [83]. The results were compared with the permeability data determined in humans [84].
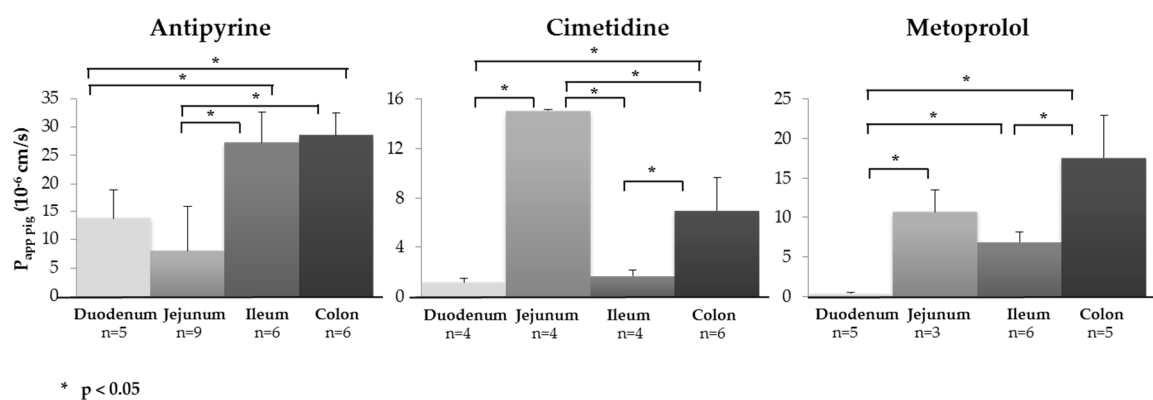

Figure 2. The porcine ex vivo model was able to identify regional variations in intestinal absorption ($P_{app,pig}$) for metoprolol, cimetidine and antipyrine in the duodenum, jejunum, ileum and colon. A 100 μM solution of each drug was prepared in KBR (Mean $\pm$ SD; n = number of replicates). A statistical analysis was performed using one-way ANOVA followed by a Bonferroni's multiple comparisons ad hoc test.

Table 3. The apparent drug permeability coefficients, $P_{app,pig}$ and Q_{DEP} and Q_{PERM}, for drugs in different segments of the small intestine (duodenum, jejunum and ileum) and the colon.

Drug	$P_{app,pig}$ Ex Vivo (10^{-6} cm/s)				Q_{DEP} (%) Q_{PERM} (%) (*n*) [a]							
	Duodenum (*n*)	Jejunum (*n*)	Ileum (*n*)	Colon (*n*)	Duodenum		Jejunum		Ileum		Colon	
Antipyrine	13.69 ± 5.24 (5)	8.06 ± 7.91 (9)	27.26 ± 5.47 (6)	28.56 ± 3.97 (6)	1.10 ± 0.47	1.57 ± 0.58 (5)	0.72 ± 0.20	2.18 ± 0.53 (5)	1.97 ± 0.34	1.39 ± 0.56 (6)	0.87 ± 0.16	3.79 ± 0.80 (5)
Cimetidine	1.12 ± 0.30 (4)	15.01 ± 0.07 (4)	1.66 ± 0.48 (4)	6.91 ± 2.74 (6)	0.67 ± 0.06	0.91 ± 0.27 (4)	3.28 ± 0.56	1.66 ± 0.64 (6)	0.07 ± 0.01	0.26 ± 0.08 (3)	0.05 ± 0.01	0.81 ± 0.25 (6)
Metoprolol	0.39 ± 0.16 (5)	10.64 ± 2.92 (3)	6.87 ± 1.23 (6)	17.55 ± 5.41 (6)	2.35 ± 0.25	0.14 ± 0.08 (5)	0.27 ± 0.04	0.18 ± 0.05 (4)	1.89 ± 0.67	0.83 ± 0.09 (5)	0.02 ± 0.00	1.65 ± 0.87 (6)

[a] Number of replicates.

In the case of antipyrine, $P_{app,pig}$ across the ileum was significantly greater than that for uptake across the duodenum and jejunum ($p < 0.05$), i.e., an improved permeation on passing from the proximal to the distal small intestine. It was noted that $P_{app,pig}$ for uptake in the colon was equivalent to that in the ileum. A similar behavior was observed with metoprolol, where a statistically significant increase in $P_{app,pig}$ from the proximal to the distal gastrointestinal tract was observed ($p < 0.05$). As mentioned above, in contrast to antipyrine and metoprolol, which are BCS I drugs, cimetidine is a BCS III drug, and it behaved differently: In this case, $P_{app,pig}$ was significantly higher in the jejunum as compared to all the other segments ($p < 0.05$).

To date, few in vivo data regarding a regional variation in drug permeability in humans are available. Of the drugs tested here, $P_{eff,human}$ has only been determined for cimetidine [85], and the same trend was observed: The $P_{eff,human}$ across jejunum was significantly higher than that across the other segments (although the absolute value of $P_{app,pig}$ was approx. 50-fold lower than (uncorrected) $P_{eff,human}$). It was found that $P_{eff,human}$ decreased three-fold going from the jejunum to the ileum (from 75×10^{-6} cm/s to 25×10^{-6} cm/s), in comparison, $P_{app,pig}$ decreased approx. eight-fold.

In terms of ex vivo data from human intestine in the Ussing chamber ($P_{app,human}$), (i) for antipyrine, the $P_{app,human}$ values increased approximately two-fold on going from the duodenum to the colon ($26.3 \pm 6.99 \times 10^{-6}$ cm/s to $54.6 \pm 13.0 \times 10^{-6}$ cm/s) [28] and were similar to $P_{app,pig}$ measured here ($13.7 \pm 5.2 \times 10^{-6}$ cm/s and $28.6 \pm 4.0 \times 10^{-6}$ cm/s, respectively); (ii) for cimetidine, $P_{app,human}$ was only determined for the jejunum ($3.74 \pm 0.47 \times 10^{-6}$ cm/s) and was approximately two-fold higher than $P_{app,pig}$ ($1.50 \pm 0.07 \times 10^{-6}$ cm/s); and (iii) for metoprolol, $P_{app,pig}$ was in the same range as $P_{app,human}$ in the jejunum ($10.64 \pm 2.92 \times 10^{-6}$ cm/s vs. $15.9 \pm 3.69 \times 10^{-6}$ cm/s, respectively) and in the colon ($17.55 \pm 5.41 \times 10^{-6}$ cm/s vs. $18.8 \pm 4.0 \times 10^{-6}$ cm/s, respectively) (Table 3) [28]. In general, there was a good agreement between $P_{app,human}$ and $P_{app,pig}$ (although $P_{app,human}$ was usually a little higher) confirming that healthy porcine intestinal tissue was able to identify regional differences in drug absorption consistent with those reported with human intestine [28].

3.3. Demonstrating Activity of the P-gp Efflux Transporter

The transport of two low permeability drugs, cimetidine and ranitidine (both BCS III), which are known substrates of P-gp [81,83,86], in the jejunum and ileum was investigated in the presence and absence of the P-gp inhibitor verapamil (Figure 3). BCS III substances were chosen since P-gp plays a minimal role in the drug permeation of high permeability drugs (BCS I and II) [87]. No statistically significant difference in $P_{app,pig}$ was observed for transport across the jejunum in the presence or absence of verapamil (Table 4). In contrast, the presence of verapamil significantly increased $P_{app,pig}$ in the ileum for both cimetidine and ranitidine. In human intestine, P-pg expression in the proximal intestine is lower than in the distal small intestine [41,84]. The more pronounced effect of verapamil on the absorption in the ileum suggested that the same P-gp distribution might be present in porcine intestine. However, since it is reported that verapamil is a modulator of the organic cation transporter, the effect—if any—of this activity needs to be investigated [88,89].

Table 4. The apparent drug permeability coefficients, $P_{app,pig}$ and Q_{DEP} and Q_{PERM}, in the jejunum and ileum for the drug substrates of the P-gp efflux transporter in the presence (+VER) and absence (−VER) of the P-gp inhibitor, verapamil.

Drug	$P_{app,pig}$ Ex Vivo (10^{-6} cm/s)				Q_{DEP} (%) Q_{PERM} (%) (n) [a]							
	Jejunum		Ileum		Jejunum		Jejunum		Ileum		Ileum	
	(−VER) (n)	(+VER) (n)	(−VER) (n)	(+VER) (n)	(−VER)		(+VER)		(−VER)		(+VER)	
Cimetidine	15.01 ± 0.07 (4)	10.07 ± 4.80 (6)	1.66 ± 0.48 (4)	4.28 ± 0.70 (4)	2.98 ± 0.29	1.38 ± 0.03 (4)	4.32 ± 0.97	1.49 ± 0.67 (6)	0.07 ± 0.01	0.26 ± 0.08 (3)	0.08 ± 0.02	0.71 ± 0.14 (4)
Ranitidine	5.42 ± 0.61 (6)	4.92 ± 0.30 (5)	1.04 ± 0.83 (5)	4.78 ± 0.31 (6)	1.32 ± 0.31	0.67 ± 0.12 (6)	5.47 ± 0.75	0.23 ± 0.15 (5)	1.10 ± 0.59	0.55 ± 0.35 (4)	7.91 ± 0.74	0.25 ± 0.03 (6)

[a] Number of replicates.
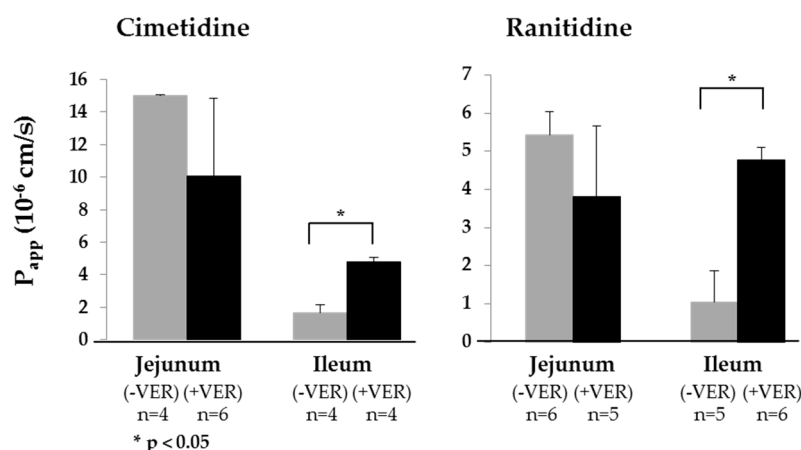
Figure 3. The activity of the P-gp efflux transporter was confirmed by measuring $P_{app,pig}$ of the P-gp substrates, cimetidine and ranitidine (both prepared at a concentration of 100 µM in KBR), in the jejunum and the ileum in the presence (+VER; 100 µM) or absence (−VER) of verapamil (a P-gp inhibitor). Statistically significant differences (Student's t-test) were observed for the ileum, which was consistent with the reports for humans in vivo. (Mean ± SD; *n* = number of replicates).

3.4. Demonstrating that CYP3A4 Retains Activity in the Porcine Intestine Ex Vivo

Another crucial process during drug permeation in vivo is the pre-systemic metabolism in the gut wall—principally due to CYP3A4 activity. To test whether CYP3A4 activity was retained in porcine intestine ex vivo, the intestinal permeation of three CYP3A4 substrates, midazolam, tamoxifen and verapamil, was investigated in the presence and absence of clotrimazole, a potent CYP3A4 inhibitor. The $P_{app,pig}$ of all three substances significantly increased in the presence of clotrimazole (Table 5); furthermore, the amount of each of the principal metabolites—α-hydroxymidazolam, N-desmethyl-tamoxifen, and norverapamil—in the intestinal tissue was significantly decreased (Figure 4).

Table 5. The apparent drug permeability coefficients, $P_{app,pig}$ and Q_{DEP} and Q_{PERM}, in the jejunum for drug substrates of CYP3A4 in the presence (+CLOTR) and absence (−CLOTR) of the CYP3A4 inhibitor, clotrimazole.

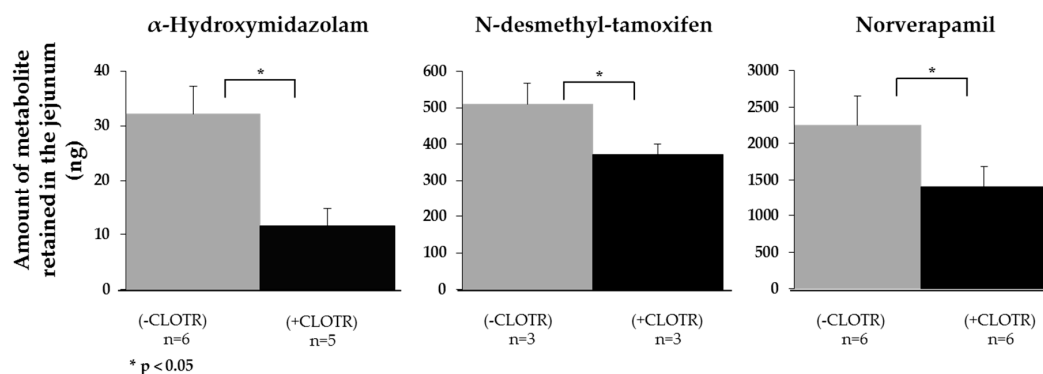| Drug	$P_{app,pig}$ Ex Vivo $(10^{-6}$ cm/s)				Q_{DEP} (%) Q_{PERM} (%) (*n*) [a]					
	(−CLOTR)	(*n*)	(+CLOTR)	(*n*)	(−CLOTR)			(+CLOTR)		
Midazolam	0.183 ± 0.138	(4)	0.460 ± 0.070	(4)	8.06 ± 1.33	0.13 ± 0.09	(6)	7.49 ± 2.50	0.18 ± 0.08	(5)
Tamoxifen	0.124 ± 0.046	(3)	1.381 ± 1.080	(3)	1.82 ± 1.39	0.07 ± 0.07	(3)	1.82 ± 0.58	0.06 ± 0.06	(4)
Verapamil	0.008 ± 0.003	(4)	0.211 ± 0.071	(3)	1.88 ± 0.12	0.00 ± 0.00	(3)	3.00 ± 0.63	0.18 ± 0.07	(6)

[a] Number of replicates.

Figure 4. The enzymatic activity of CYP3A4 in the intestinal tissue was confirmed by investigating the transport of the CYP3A4 substrates midazolam, tamoxifen and verapamil (all prepared at a concentration of 100 μM in KBR) across the jejunum and quantification of the amounts (of their metabolites (α-hydroxymidazolam, N-desmethyl-tamoxifen and norverapamil) retained in the tissue in the presence (+CLOTR; 100 μM) or absence (−CLOTR) of the CYP3A4 inhibitor clotrimazole. Statistically significant differences were identified using the Student's t-test. (Mean ± SD; *n* = number of replicates).

3.5. Relative Contribution of Drug Deposition (Q_{DEP}) and Drug Permeation (Q_{PERM}) to the Transport Index (TI)

The values of Q_{DEP} and Q_{PERM} provide insight at a number of levels (Table 2). First, Q_{DEP} reports on the fraction of drugs that partitioned from the formulation in the donor compartment into the intestinal tissue but was unable to reach the receiver compartment within the timeframe of the permeation experiment. Thus, it is not taken into account in the calculations that measure the permeability coefficient and, hence, may contribute to the underestimation of intestinal absorption ex vivo. Second, the relative magnitudes of Q_{DEP} and Q_{PERM} reflect the effect of the drug physicochemical properties on molecular transport into and across the intestine (Tables 1 and 2). Highly lipophilic molecules, e.g., midazolam, tamoxifen and verapamil, used in the studies to investigate CYP3A4 activity showed a clear trend towards accumulation within the membrane. In a similar way, the moderately lipophilic character of ketoprofen and piroxicam may explain their retention within the intestinal tissue. Although the P-gp substrates, cimetidine and ranitidine, are significantly more polar, they demonstrated a selectivity for membrane accumulation over permeation; this was tentatively attributed to their capacity to form hydrogen bonds (HB): They both contained five HB acceptor groups in addition to multiple HB donor functions—three in the case of cimetidine and two for ranitidine. The relative values of Q_{DEP} and Q_{PERM} for metoprolol and, in particular, atenolol were more difficult to explain. In the case of metoprolol, a combination of modest lipophilicity and HB formation capacity (four HB acceptors and two HB donors) might be sufficient to account for its behavior. Atenolol was more polar but contained four HB acceptors and two HB donors. It was noted that most of the molecules with a propensity to accumulate were P-gp substrates, although whether and/or how this might influence retention is unclear at this point. Regional differences in the relative magnitudes of Q_{DEP} and Q_{PERM} were observed: The Q_{PERM}/Q_{DEP} ratio was significantly greater in the colon for antipyrine, cimetidine and metoprolol than in the small intestine.

In the case of the CYP3A4 substrates, the presence of clotrimazole only had a statistically significant effect on the Q_{DEP} and Q_{PERM} of verapamil ($p < 0.05$ and $p < 0.05$, respectively). As shown in Figure 4, during the permeation experiment, the metabolite norverapamil was formed, which is itself a strong CYP3A4 inhibitor [89]. CYP3A4 inhibition by clotrimazole in conjunction with norverapamil may have helped to increase the amount of verapamil in the tissue, which accumulated due to its lipophilicity.

4. Conclusions

The results demonstrated that viable porcine intestine ex vivo could be used in conjunction with an Ussing chamber system to evaluate the effect of physiological conditions on intestinal drug absorption. The comparison of passive drug absorption from KBR and with biorelevant media simulating fasted and fed states was a step forward in trying to predict drug absorption under more physiological conditions. An excellent correlation was observed between $P_{app,pig}$ and the drug permeability coefficient, $P_{eff,human}$, measured in vivo both in terms of the trend and absolute values once a correction was made to take into account the actual surface area for absorption in vivo [77]. The experiments investigating the differences in regional/segmental uptake demonstrated the potential of the model to aid in the rational design of formulations that enabled release in the region with the highest drug permeability. The advantages of using viable tissue were clearly shown in the studies illustrating the impact of P-gp transport and pre-systemic metabolism by CYP3A4 present in the gut wall. From an ethical standpoint, the technique had the advantage in that it did not require the sacrifice of any animals in the laboratory. Furthermore, healthy tissue was sourced from a large omnivorous mammal. In the next phase of the project, the aims are (i) to create a dynamic system that mimics molecular transit through the different compartments of the gastrointestinal tract and which enables the direct evaluation of oral drug dosage forms and (ii) to explore the potential applications in food and nutrition and the elucidation of active compounds present in complex formulations used in traditional medicine.

References

1. Rogers, S.M.; Back, D.J.; Orme, M.L.E. Intestinal metabolism of ethinyloestradiol and paracetamol in vitro: Studies using Ussing chambers. *Br. J. Clin. Pharmacol.* **1987**, *23*, 727–734. [CrossRef] [PubMed]
2. Arnold, Y.E.; Imanidis, G.; Kuentz, M.T. Advancing in-vitro drug precipitation testing: New process monitoring tools and a kinetic nucleation and growth model. *J. Pharm. Pharmacol.* **2011**, *63*, 333–341. [CrossRef] [PubMed]
3. Cohen, J.L.; Hubert, B.B.; Leeson, L.J.; Rhodes, C.T.; Robinson, J.R.; Roseman, T.J.; Shefter, E. The development of USP dissolution and drug release standards. *Pharm. Res.* **1990**, *7*, 983–987. [CrossRef]
4. Minekus, M.; Marteau, P.; Havenaar, R.; Huis, J.H.J. A multicompartmental dynamic computer-controlled model simulating the stomach and small intestine. *Altern. Lab. Anim. ATLA* **1995**, *23*, 197–209.
5. Barker, R.; Abrahamsson, B.; Kruusmaegi, M. Application and validation of an advanced gastrointestinal in vitro model for the evaluation of drug product performance in pharmaceutical development. *J. Pharm. Sci.* **2014**, *103*, 3704–3712. [CrossRef]
6. Blanquet, S.; Zeijdner, E.; Beyssac, E.; Meunier, J.-P.; Denis, S.; Havenaar, R.; Alric, M. A dynamic artificial gastrointestinal system for studying the behavior of orally administered drug dosage forms under various physiological conditions. *Pharm. Res.* **2004**, *21*, 585–591. [CrossRef] [PubMed]

7.	Arnold, Y.; Bravo Gonzalez, R.; Versace, H.; Kuentz, M. Comparison of different in vitro tests to assess oral lipid-based formulations using a poorly soluble acidic drug. *J. Drug Del. Sci. Technol.* **2010**, *20*, 143–148. [CrossRef]

8.	Walter, E.; Janich, S.; Roessler, J.; Hilfinger, J.; Amidon, G. H29-MTX/Caco-2 cocultures as an in vitro model for the intestinal epithelium: In vitro-in vivo correlation with permeabiltiy data from rats and humans. *J. Pharm. Sci.* **1996**, *85*, 1070–1076. [CrossRef]

9.	Hilgendorf, C.; Spahn-Langguth, H.; Regardh, C.; Lipka, E.; Amidon, G.; Langguth, P. Caco-2 versus Caco-2/HT29-MTX co-cultured cell lines: Permeabilities via diffusion, inside- and outside-directed carrier-mediated transport. *J. Pharm. Sci.* **2000**, *89*, 63–75. [CrossRef]

10.	Araujo, F.; Sarmento, B. Towards the characterization of an in vitro triple co-culture intestine cell model for permeability studies. *Int. J. Pharm.* **2013**, *458*, 128–134. [CrossRef] [PubMed]

11.	Lozoya-Agullo, I.; Araujo, F.; Gonzalez-Alvarez, I.; Merino-Sanjuan, M.; Gonzalez-Alvarez, M.; Bermejo, M.; Sarmento, B. Usefulness of Caco-2/HT29-MTX and Caco-2/HT29-MTX/Raji B coculture models to predict intestinal and colonic permeability compared to Caco-2 monoculture. *Mol. Pharm.* **2017**, *14*, 1264–1270. [CrossRef] [PubMed]

12.	Wuyts, B.; Riethorst, D.; Brouwers, J.; Tack, J.; Annaert, P.; Augustijns, P. Evaluation of fasted satte human intestinal fluid as apical solvent system in the Caco-2 absoprtion model and comparison with FaSSIF. *Eur. J. Pharm. Sci.* **2015**, *67*, 126–135. [CrossRef]

13.	Antoine, D.; Pellequer, Y.; Tempesta, C.; Lorscheidt, S.; Kettel, B.; Tamaddon, L.; Jannin, V.; Demarne, F.; Lamprecht, A.; Béduneau, A. Biorelevant media resistant co-culture model mimicking permeability of human intestine. *Int. J. Pharm.* **2015**, *481*, 27–36. [CrossRef]

14.	Lozoya-Agullo, I.; Gonzalez-Alvarez, I.; Zur, M.; Fine-Shamir, N.; Cohen, Y.; Markovic, M.; Garrigues, T.M.; Dahan, A.; Gonzalez-Alvarez, M.; Merino-Sanjuan, M.; et al. Closed-loop Doluisio (colon, small intestine) and single-pass intestinal perfusion (colon, jejunum) in rat-biophysical model and predictions based on Caco-2. *Pharm. Res.* **2018**, *2018*, 2–23. [CrossRef]

15.	Mani, V.; Hollis, J.H.; Gabler, N.K. Dietary oil composition differentially modulates intestinal endotoxin transport and postprandial endotoxemia. *Nutr. Metab.* **2013**, *10*, 1–9. [CrossRef]

16.	Kansara, V.; Mitra, A.K. Evaluation of an ex vivo model implication for carrier-mediated retinal drug delivery. *Curr. Eye Res.* **2006**, *31*, 415–426. [CrossRef]

17.	Eisenhut, M. Changes in ion transport in inflammatory disease. *J. Inflamm.* **2006**, *3*. [CrossRef]

18.	Burshtein, G.; Friedman, M.; Greenberg, S.; Amnon, H. Transepithelial transport of a natural cholinesterase inhibitor, huperzine A, along the gastrointestinal tract: The role of ionization on absorption mechanism. *Planta Med.* **2013**, *79*, 259–265. [CrossRef]

19.	Jin, L.; Boyd, B.J.; White, P.J.; Pennington, M.W.; Norton, R.S.; Nicolazzo, J.A. Buccal mucosal delivery of a potent peptide leads to therapeutically-relevant plasma concentrations for the treatment of autoimmune diseases. *J. Control. Release* **2015**, *199*, 37–44. [CrossRef]

20.	Boudry, G. The Ussing chamber technique to evaluate alternatives to in-feed antibiotics for young pigs. *Anim. Res.* **2005**, *54*, 219–230. [CrossRef]

21.	Ussing, H.H.; Zerahn, K. Active transport of sodium as the source of electric current in the short-circuited isolated frog skin. *Acta Physiol. Scand.* **1951**, *23*, 110–127. [CrossRef] [PubMed]

22.	Wu-Pong, S.; Livesay, V.; Dvorchik, B.; Barr, W.H. Oligonucleotide transport in rat and human intestine Ussing chamber models. *Biopharm. Drug Dispos.* **1999**, *20*, 411–416. [CrossRef]

23.	Nejdfors, P.; Ekelund, M.; Jeppson, B.; Weström, B.R. Mucosal in vitro permeability in the intestinal tract of the pig, the rat, and man: Species- and region-related differences. *Scand. J. Gastroenterol.* **2000**, *35*, 501–507. [PubMed]

24.	Ungell, A.-L.; Nylander, S.; Bergstrand, S.; Sjöberg, A.; Lennernäs, H. Membrane transport of drugs in different regions of the intestinal tract of the rat. *J. Pharm. Sci.* **1998**, *87*, 360–366. [CrossRef]

25.	Haslam, I.S.; O'Reilly, D.A.; Sherlock, D.J.; Kauser, A.; Womack, C.; Coleman, T. Pancreatoduodenectomy as a source of human small intestine for Ussing chamber investigations and comparative studies with rat tissue. *Biopharm. Drug Dispos.* **2011**, *32*, 210–221. [CrossRef]

26.	Rozehnal, V.; Nakai, D.; Hoepner, U.; Fischer, T.; Kamiyama, E.; Takahashi, M.; Mueller, J. Human small intestinal and colonic tissue mounted in the Ussing chamber as a tool for characterizing the intestinal absorption of drugs. *Eur. J. Pharm. Sci.* **2012**, *46*, 367–373. [CrossRef] [PubMed]

27. Miyake, M.; Toguchi, H.; Nishibayashi, T.; Higaki, K.; Sugita, A.; Koganei, K.; Kamada, N.; Kitazume, M.T.; Hisamatsu, T.; Sato, T.; et al. Establishment of novel prediction system of intestinal absorption in humans using human intestinal tissue. *J. Pharm. Sci.* **2013**, *102*, 2564–2571. [CrossRef]

28. Sjöberg, A.; Lutz, M.; Tannergren, C.; Wingolf, C.; Borde, A.; Ungell, A.-L. Comprehensive study on regional human intestinal permeability and prediction of fraction absorbed of drugs using the Ussing chamber technique. *Eur. J. Pharm. Sci.* **2013**, *48*, 166–180. [CrossRef]

29. Söderholm, J.D.; Hedman, L.; Artursson, P.; Franzén, L.; Larsson, J.; Pantzar, N.; Permert, J.; Olaison, G. Integrity and metabolism of human ileal mucosa in vitro in the Ussing chamber. *Acta Physiol. Scand.* **1998**, *162*, 47–56. [CrossRef]

30. Menon, R.M.; Barr, W.H. Comparison of ceftibuten transport across Caco-2 cells and rat jejunum mounted on modified Ussing chambers. *Biopharm. Drug Dispos.* **2003**, *24*, 299–308. [CrossRef]

31. Kim, J.-S.; Mitchell, S.; Kijek, P.; Tsume, Y.; Hilfinger, J.; Amidon, G.L. The suitability of an in situ perfusion model for permeability determinations: Utility for BCS Class I biowaiver requests. *Mol. Pharm.* **2006**, *3*, 686–694. [CrossRef] [PubMed]

32. Lennernäs, H. Animal data: The contributions of the Ussing chamber and perfusion systems to predicting human oral drug delivery in vivo. *Adv. Drug Deliver. Rev.* **2007**, *59*, 1103–1120. [CrossRef]

33. Kararli, T.T. Comparison of the gastrointestinal anatomy, physiology, and biochemistry of humans and commonly used laboratory animals. *Biopharm. Drug Dispos.* **1995**, *16*, 351–380. [CrossRef] [PubMed]

34. Sjoegren, E.; Abrahamsson, B.; Augustijns, P.; Becker, D.; Bolger, M.B.; Brewster, M.; Brouwers, J.; Flanagan, T.; Harwood, M.; Heinen, C.; et al. In vivo methods for drug absorption—Comparative physiologies, model selection, correlation with in vitro methods (IVIC), and applications for formulation/API/excipient characterization including food effects. *Eur. J. Pharm. Sci.* **2014**, *57*, 99–151. [CrossRef] [PubMed]

35. Patterson, J.K.; Lei, X.G.; Miller, D.D. The pig as an experimental model for elucidation the mechanisms governing dietary influence on mineral absorption. *Exp. Bio. Med.* **2008**, *233*, 651–664. [CrossRef] [PubMed]

36. Musther, H.; Olivares-Morales, A.; Hatley, O.J.D.; Liu, B.; Hodjegan, A.R. Animal versus human oral drug bioavailability: Do they correlate? *Eur. J. Pharm. Sci.* **2014**, *57*, 280–291. [CrossRef] [PubMed]

37. Miller, E.; Ullrey, D. The pig as a model for human nutrition. *Ann. Rev. Nutr.* **1987**, *7*, 361–382. [CrossRef]

38. Witkamp, R.; Monshouwer, M. Pharmacokinetics in vivo and in vitro in swine. *Scan. J. Lab. Anim. Sci.* **1998**, *25*, 45–56.

39. Skaanild, M. Porcine cytochrome P450 and metabolism. *Curr. Pharm. Des.* **2006**, *12*, 1421–1427. [CrossRef] [PubMed]

40. Schrickx, J. *ABC-Transporters in the Pig*; Faculty of Veterinary Medicine, Utrecht University: Utrecht, The Netherlands, 2006.

41. Mouly, S.; Paine, M.F. P-glyocportein increases from proximal to distal regions of human small intestine. *Pharm. Res.* **2003**, *20*, 1595–1599. [CrossRef] [PubMed]

42. Tang, H.; Pak, Y.; Mayersohn, M. Protein expression pattern of p-glycoprotein along the gastrointestinal tract of the yucatan micropig. *J. Biochem. Mol. Toxicol.* **2004**, *18*, 18–22. [CrossRef] [PubMed]

43. Deusser, H.; Rogoll, D.; Scheppach, W.; Volk, A.; Melcher, R.; Richling, E. Gastrointestinal absorption and metabolism of apple polyphenols ex vivo by the pig intestinal mucosa in the Ussing chamber. *Biotechnol. J.* **2013**, *8*, 363–370. [CrossRef]

44. Erk, T.; Hauser, J.; Williamson, G.; Renouf, M.; Steiling, H.; Dionisi, F.; Richling, E. Structure- and dose-absorption relationships of coffee polyphenols. *Biofactors* **2013**, *40*, 103–112. [CrossRef]

45. Westerhout, J.; van de Steeg, A.; Grossouw, D.; Zeijdner, E.E.; Krul, C.A.M.; Verwei, M.; Wortelboer, H.M. A new approach to predict human intestinal absorption using porcine intestinal tissue and biorelevant matrices. *Eur. J. Pharm. Sci.* **2014**, *63*, 167–177. [CrossRef]

46. Neirinckx, E.; Vervaet, C.; Michiels, J.; De Smet, S.; Van den Broeck, W.; Remon, J.P.; De Backer, P.; Croubels, S. Feasibility of the Ussing chamber technique for the determination of in vitro jejunal permeability of passively absorbed compounds in different animal species. *J. Vet. Pharmacol. Therap.* **2010**, *34*, 290–297. [CrossRef]

47. Herrmann, J.; Hermes, R.; Breves, G. Transepithelial transport and intraepithelial metabolism of short-chain fatty acids (SCFA) in the porcine proximal colon are influenced by SCFA concentration and luminal pH. *Comp. Biochem. Physiol. A Mol. Integr. Physiol.* **2011**, *158*, 169–176. [CrossRef]

48. Lampen, A.; Zhang, Y.; Hackbarth, I.; Benet, L.Z.; Sewig, K.-F.; Christians, U. Metabolism and transport of the macrolide immunosuppressant sirolimus in the small intestine. *J. Pharmcol. Exp. Ther.* **1998**, *285*, 1104–1112.

49. Lampen, A.; Christians, U.; Gonschior, A.-K.; Bader, A.; Hackbarth, I.; von Engelhardt, W.; Sewing, K.-F. Metabolism of the macrolide immunosuppressant, tacrolimus, by the pig gut mucosa in the Ussing chamber. *Br. J. Pharmacol.* **1996**, *117*, 1730–1734. [CrossRef]

50. Aucamp, M.; Odendaal, R.; Wilna, L.; Hamman, J. Amorphous azithromycin with improved aqueous solubility and intestinal membrane permeability. *Drug Dev. Ind. Pharm.* **2015**, *41*, 1100–1108. [CrossRef]

51. Atlabachew, M.; Combrinck, S.; Viljoen, A.M.; Hamman, J.H.; Gouws, C. Isolation and in vitro permeation of phenylpropylamino alkaloids from Khat (*Catha edulis*) across oral and intestinal mucosal tissues. *J. Ethnopharmacol.* **2016**, *194*, 307–315. [CrossRef]

52. De Bruyn, S.; Willers, C.; Steyn, D.; Steenekamp, J.; Hamman, J. Development and evaluation of double-phase multiple-unit dosage form for enhanced insulin intestinal delivery. *Drug Deliv. Lett.* **2018**, *8*, 52–60. [CrossRef]

53. Gerber, W.; Hamman, J.H.; Steyn, J.D. Excipient-drug pharmacokinetic interactions: Effect of disintegrants on efflux across excised pig intestinal tissues. *J. Food Drug Anal.* **2018**, *26*, S115–S124. [CrossRef] [PubMed]

54. Pietzonka, P.; Walter, E.; Duda-Johner, S.; Langguth, P.; Merkle, H.P. Compromised integrity of excised porcine intestinal epithelium obtained from the abattoir affects the outcome of in vitro particle uptake studies. *Eur. J. Pharm. Sci.* **2002**, *15*, 39–47. [CrossRef]

55. Shikanga, E.A.; Hamman, J.H.; Chen, W.; Combrinck, S.; Gericke, N.; Viljoen, A.M. In vitro permeation of mesembrine alkaloids from *Sceletium tortuosum* across porcine buccal, sublingual, and intestinal mucosa. *Planta Med.* **2012**, *78*, 260–268. [CrossRef] [PubMed]

56. Hoegman, M.; Moerk, A.-C.; Roomans, G.M. Hypertonic saline increases tight junction permeability in airway epithelium. *Eur. Respir. J.* **2002**, *20*, 1444–1448. [CrossRef]

57. Clark, L.L. A guide to Ussing chamber studies of mouse intestine. *Am. J. Physiol. Gastrointest. Liver Physiol.* **2009**, *296*, G1151–G1166. [CrossRef] [PubMed]

58. Jantratid, E.; Niels, J.; Reppas, C.; Dressman, J.B. Dissolution media simulating conditions in the proximal human gastrointestinal tract: An update. *Pharm. Res.* **2008**, *25*, 1663–1676. [CrossRef] [PubMed]

59. Winiwarter, S.; Bonham, N.M.; Ax, F.; Hallberg, A.; Lennernäs, H.; Karlén, A. Correlation of human jejunal permeability (in vivo) of drugs with experimentally and theoretically derived parameters. A multivariate data analysis approach. *J. Med. Chem.* **1998**, *41*, 4934–4949. [CrossRef]

60. Sarti, F.; Müller, C.; Iqbal, J.; Perera, G.; Laffleur, F.; Bernkop-Schnürch, A. Development and in vivo evaluation of an oral vitamin B12 delivery system. *Eur. J. Pharm. Biopharm.* **2013**, *84*, 132–137. [CrossRef]

61. Zhang, W.; Ramamoorthy, Y.; Kilicarslan, T.; Nolte, H.; Tyndale, R.F.; Sellers, E.M. Inhibition of cytochromes P450 by antifungal imidazole derivatives. *Drug Metab. Dispos.* **2002**, *30*, 314–318. [CrossRef]

62. Artursson, P. Epithelial transport of drugs in cell culture. I: A model for studying the passive diffusion of drugs over intestinal absorbtive (Caco-2) cells. *J. Pharm. Sci.* **1990**, *79*, 476–482. [CrossRef] [PubMed]

63. Cazares-Delgadillo, J.; Naik, A.; Ganem-Rondero, A.; Quintanar-Guerrero, D.; Kalia, Y. Transdermal delivery of Cytochrome C—A 12.4 kDa protein-across intact skin by constant-current iontophoresis. *Pharm. Res.* **2007**, *24*, 1360–1368. [CrossRef] [PubMed]

64. Yu, J.; Kalaria, D.R.; Kalia, Y.N. Erbium: YAG fractional laser ablation for the percutaneous delivery of intact functional therapeutic antibodies. *J. Control. Release* **2011**, *156*, 53–59. [CrossRef]

65. Lapteva, M.; Mondon, K.; Moller, M.; Gurny, R.; Kalia, Y.N. Polymeric micelle nanocarriers for the cutaneous delivery of tacrolimus: A targeted approach for the treatment of psoriasis. *Mol. Pharm.* **2014**, *11*, 2989–3001. [CrossRef] [PubMed]

66. Chen, Y.; Kalia, Y.N. Short-duration ocular iontophoresis of ionaziable aciclovir prodrugs: A new approach to treat herpes simplex infections in the anterior and posterior segments of the eye. *Int. J. Pharm.* **2018**, *536*, 292–300. [CrossRef]

67. Miyake, M.; Kondo, S.; Koga, T.; Yoda, N.; Nakazato, S.; Emoto, C.; Mukai, T.; Toguchi, H. Evaluation of intestinal metabolism and absorption using Ussing chamber system, equipped with intestinal tissue from rats and dogs. *Eur. J. Pharm. Biopharm.* **2018**, *122*, 49–53. [CrossRef]

68. Bachhav, Y.G.; Heinrich, A.; Kalia, Y.N. Using laser microporation to improve transdermal deliveriy of diclofenac: Increasing bioavailability and the range of therapeutic applications. *Eur. J. Pharm. Biopharm.* **2011**, *78*, 408–414. [CrossRef]

69. Kalaria, D.R.; Patel, P.; Merino, V.; Patravale, V.B.; Kalia, Y.N. Controlled iontophoretic transport of huperzine A across skin in vitro and in vivo: Effect of delivery conditions and comparison of pharmacokinetic models. *Mol. Pharm.* **2013**, *10*, 4322–4329. [CrossRef]

70. Kalaria, D.R.; Patel, P.; Merino, V.; Patravale, V.B.; Kalia, Y.N. Controlled iontophoretic delivery of pramipexole: Electrotransport kinetics in vitro and in vivo. *Eur. J. Pharm. Biopharm.* **2014**, *88*, 56–63. [CrossRef]

71. Dressman, J.B.; Amidon, G.L.; Reppas, C.; Shah, V.P. Dissolution testing as a prognostic tool for oral drug absorption: Immediate release dosage forms. *Pharm. Res.* **1998**, *15*, 11–22. [CrossRef]

72. Ingels, F.; Deferme, S.; Destexhe, E.; Oth, M.; Van den Mooter, G.; Augustijns, P. Simulated intestinal fluid as transport medium in the Caco-2 cell culture model. *Int. J. Pharm.* **2002**, *232*, 183–192. [CrossRef]

73. Patel, N.; Forbes, B.; Eskola, S.; Murray, J. Use of simulated intestinal fluids with Caco-2 cells. *Drug Dev. Ind. Pharm.* **2006**, *32*, 151–161. [CrossRef] [PubMed]

74. Lind, M.L.; Jacobsen, J.; Holm, R.; Müllertz, A. Development of simulated intestinal fluids containing nutrients as transport media in the Caco-2 cell culture model: Assessment of cell viability, monolayer integrity and transport of poorly aqueous soluble drug and a substrate of efflux mechanisms. *Eur. J. Pharm. Sci.* **2007**, *32*, 261–270. [CrossRef] [PubMed]

75. Markopoulos, C.; Thoenen, F.; Preisig, D.; Symillides, M.; Vertzoni, M.; Parrott, N.; Reppas, C.; Imanidis, G. Biorelevant media for transport experiments in the Caco-2 model to evaluate drug absorption in the fasted and the fed state and their usefulness. *Eur. J. Pharm. Biopharm.* **2014**, *86*, 438–448. [CrossRef] [PubMed]

76. Knutson, L.; Odlind, B.; Hällgren, R. A new technique for segmental jejunal perfusion in man. *Am. J. Gastroenterol.* **1989**, *84*, 1278–1284.

77. Olivares-Morales, A.; Lennernaes, H.; Aarons, L.; Rostami-Hodjegan, A. Translating human effective jejunal intestinal permeability to surface-dependent intrinsic permeability: A pragmatic method for a more mechanistic prediction of regional oral drug absorption. *AAPS J.* **2015**, *17*, 1177–1192. [CrossRef]

78. Lennernäs, H. Human intestinal permeability. *J. Pharm. Sci.* **1998**, *87*, 403–410. [CrossRef]

79. Miller, J.M.; Beig, A.; Krieg, B.J.; Carr, R.A.; Borchardt, T.B.; Amidon, G.E.; Amidon, G.L.; Dahan, A. The solubility-permeability interplay: Mechanistic modeling and predicitive application of the impact of micellar solubilization on intestinal permeation. *Mol. Pharm.* **2011**, *8*, 1848–1856. [CrossRef]

80. Yano, K.; Masaoka, Y.; Kataoka, M.; Sakuma, S.; Yamashita, S. Mechanisms of membrane transport of poorly soluble drugs: Role of micelles in oral absorption processes. *J. Pharm. Sci.* **2010**, *99*, 1336–1345. [CrossRef]

81. Tannergren, C.; Bergendal, A.; Lennernäs, H.; Abrahamsson, B. Toward an increased understanding of the barriers to colonic drug absorption in humans: Implication for early controlled release candidate assessment. *Mol. Pharm.* **2009**, *6*, 60–73. [CrossRef]

82. Lennernäs, H.; Palm, K.; Fagerholm, U.; Artursson, P. Comparison between active and passive drug transport in human intestinal epithelial (Caco-2) cells in vitro and human jejunum in vivo. *Int. J. Pharm.* **1996**, *127*, 103–107. [CrossRef]

83. Collett, A.; Higgs, N.B.; Sims, M.; Rowland, M.; Warhurst, G. Modulation of the permeability of H_2 receptor antagonists cimetidine and ranitidine by p-glycoprotein in rat intestine and the human colonic cell line Caco-2. *J. Pharmacol. Exp. Ther.* **1999**, *288*, 171–178. [PubMed]

84. Dahlgren, D.; Roos, C.; Sjögren, E.; Lennernäs, H. Direct in vivo human intestinal permeability (Peff) determined with different clinical perfusion and intubation methods. *J. Pharm. Sci.* **2015**, *104*, 2702–2726. [CrossRef]

85. Lennernäs, H. Regional intestinal drug permeation: Biopharmaceutics and drug development. *Eur. J. Pharm. Sci.* **2014**, *57*, 333–341. [CrossRef] [PubMed]

86. Ashmawy, S.M.; El-Gizawy, S.A.; El Maghraby, G.M.; Osman, M.A. Regional difference in intestinal drug absorption as a measure for the potential effect of P-glycoprotein efflux transporters. *J. Pharm. Pharmacol.* **2019**, *71*, 362–370. [CrossRef] [PubMed]

87. Cao, X.; Gibbs, S.T.; Fang, L.; Miller, H.A.; Landowski, C.P.; Shin, H.-C.; Lennernas, H.; Zhing, Y.; Amidon, G.L.; Yu, L.X.; et al. Why is it challenging to predict intestinal drug absorption and oral bioavailability in human using rat model. *Pharm. Res.* **2006**, *28*, 1675–1686. [CrossRef] [PubMed]

88. Salomon, J.J.; Hagos, Y.; Petzke, S.; Kühne, A.; Gausterer, J.C.; Hosoya, K.-I.; Ehrhardt, C. Beta-2 adrenergic agonists are substrates and inhibitors of human organic cation transporter 1. *Mol. Pharm.* **2015**, *12*, 2633–2641. [CrossRef] [PubMed]

89. Wang, Y.-H.; Jones, D.R.; Hall, S.D. Differential mechanism-based inhibition of CYP3A4 and CYP3A5 by verapamil. *Drug Metab. Dispos.* **2005**, *33*, 664–671. [CrossRef] [PubMed]